Archives of Toxicology

Bilirubin disrupts calcium homeostasis in neonatal hippocampal neurons: A new pathway of neurotoxicity

--Manuscript Draft--

Manuscript Number:	ATOX-D-19-00857R1
Full Title:	Bilirubin disrupts calcium homeostasis in neonatal hippocampal neurons: A new pathway of neurotoxicity
Article Type:	Original Article
Corresponding Author:	Cristina Bellarosa Fondazione Italiana Fegato ONLUS ITALY
Corresponding Author Secondary Information:	
Corresponding Author's Institution:	Fondazione Italiana Fegato ONLUS
Corresponding Author's Secondary Institution:	
First Author:	Rossana Rauti
First Author Secondary Information:	
Order of Authors:	Rossana Rauti
	Mohammed Qaisiya
	Claudio Tiribelli
	Laura Ballerini
	Cristina Bellarosa
Order of Authors Secondary Information:	
Funding Information:	
Abstract:	Severe hyperbilirubinemia leads to bilirubin encephalopathy in neonates, causing irreversible neurological sequelae. We investigated the nature of neuronal selective vulnerability to unconjugated bilirubin (UCB) toxicity. The maintenance of intracellular calcium homeostasis is crucial for neuron survival. Calcium release from endoplasmic reticulum (ER) during ER-stress can lead to apoptosis trough the activation of Caspase-12. By live calcium imaging we monitored the generation of calcium signals in dissociated hippocampal neurons and glial cells exposed to increasing UCB concentrations. We showed the ability of UCB to alter intracellular calcium homeostasis, inducing the appearance of repetitive intracellular calcium oscillations. The contribution of intracellular calcium stores and the induction and activation of proteins involved in the apoptotic calcium-dependent signaling were also assessed .Thapsigargin, a specific inhibitor of Sarco/endoplasmic reticulum ATPase (SERCA) pumps, significantly reduced the duration of Ca^{2+} oscillation associated with UCB exposure indicating that UCB strongly interfered with the reticulum calcium stores. On the contrary, in pure astrocyte cultures, spontaneous Ca^{2+} transient duration was not altered by UCB. The protein content of GRP78, AT6, CHOP, Calpain and Caspase-12 of neuronal cells treated with UCB for 24h was at least 2-fold higher compared to controls. Calcium-dependent Calpain and Caspase-12 induction by UCB were significantly reduced by 50% and 98% respectively when cells were pretreated with the ER-stress inhibitor 4-PBA. These results show the strong and direct interference of UCB with neuronal intracellular Ca^{2+} dynamics, suggesting ER Ca^{2+} stores as a primary target of UCB toxicity with the activation of the apoptotic ER-stress-dependent pathway.
Response to Reviewers:	Dear Editor, First, we would like to thank you and the reviewers for the time spent looking over the

paper. Based on the evaluation of our manuscript “Bilirubin disrupts calcium homeostasis in neonatal hippocampal neurons: A new pathway of neurotoxicity” (ATOX-D-19-00857), we submit a revised version of the Ms. together with a rebuttal letter dealing with the points raised by the reviewer

Reviewer comments (R) are in blue italic while our answers (A) are in black and include the modifications on the revised version of the manuscript. Modifications in the manuscript are highlighted in yellow.

R1. The investigators note that similar effects on calcium dynamics were observed across the original three bilirubin concentrations studied (40 NM, 90 NM, and 140 NM) - whereas the 90 and 140 nM are in the putative toxic range; 40 nM is characterized as "non-toxic" yet had effects similar to those of higher levels -- can the authors please address this observation and how it may impact the assertion that these effect on Ca dynamics are pathologic?

A1: The point raised by the reviewer is well taken. We were also surprised to observe alterations of calcium dynamics at Bf 40 nM, a concentration assumed to be not toxic. The assumption that the threshold of bilirubin toxicity is 70 nM is based on in vitro experiments (Ostrow JD, 2003, Pediatr Res 54:98–104). The validity of what observed in vitro to the ex vivo models (in this case) needs to be proven. In addition, Bf determination is influenced by the presence of many factors (FBS, HSA, BSA, chloride, pH) that changes among cell medium used to growth different primary or immortalized cell line. Bf should be measured every time in the same media used experimentally for each different cell type used (Roca L, 2006, Pediatr Res. Dec;60(6):724-8.) but this is not common practice. The Bf effect reflects differences in cell type, maturity, function, species of origin. Even if we do not have a clear explanation regarding the Bf 40 nM ability to disrupt calcium homeostasis, we believe that is important to consider that this work was conducted on dissociated primary hippocampal cells from P2-P3 Wistar rats that may be a very sensitive model.

R2. Were these changes in bilirubin-induced Ca dynamics reversible with removal - clearance of bilirubin?
A2: To answer this relevant observation from the reviewer, we have now included in the Supplementary Figure 1S results from a series of experiments where the Ca++ dynamics during bilirubin application and, upon bilirubin removal, washout was monitored for the three different bilirubin concentrations tested. As depicted by the fluorescent traces and summarized in the histograms, 5 min washout did not affected the Ca++ dynamics brought about by 10 min bilirubin application, for all concentrations tested (Bf 40 nM: from 42 ± 6 s to 37 ± 10 s, after 5 min removal, n = 5 cells; Bf 90 nM: from 54 ± 8 s to 51 ± 8 s, after 5 min removal, n= 5 cells; Bf 140 nM: from 50 ± 6 s to 42 ± 8 s, after 5 min removal, n= 4 cells). Conversely, upon 10 min bilirubin washout, a decrease in the Ca++ events’ duration was detected (Bf 40 nM: 11 ± 10 s, n = 5 cells; Bf 90 nM: 22 ± 8 s, n = 5 cells; Bf 140 nM: 27 ± 8 s, n= 5 cells), suggestive of a progressive clearance of bilirubin, with the Ca++ event duration resembling that of controls (i.e. prior bilirubin application; see for example Fig 1A or Fig 2A).

R3. Where other concentrations (lower than 40; and higher than 140 nM) studied; how about longer duration of exposures? The in vitro UCB exposures on Ca transients were 40 minutes whereas UCB effects on Ca dependent apoptotic signaling was 24 hours -- why the different time frames of exposure? How does this impact interpretation of findings?
A3: We did not test concentration lower than 40 or higher that 140 nM. As a pilot study we explored the “canonical Bf concentration” but we agree this will be informative and plan to do it in the future. The reason of the different time frames of exposure deals with the timing of events. Calcium release is a very early and rapid event, while its effect in terms of RNA and protein expression needs a longer time. 24hours is usually considered a good frame time to study RNA and protein expression.

R4. Do the authors have an explanation for the cell specific responses of UCB on Ca transients?
A4: The different impact of UCB on Ca transients between neuronal and glial cells fits with the different toxic effect of UCB in neurons and glial cells. The observation that in astrocytes, the spontaneous glial Ca2+ transients duration was not altered by UCB is

	in line with our previous demonstration that ER-stress does not occur in U87 astrocytoma cell line despite a intracellular UCB accumulation similar to neuronal cells (15). R5. Could the authors add a figure detailing the proposed pathophysiology of UCB on neuronal cell Ca dynamics and downstream effects? Would be helpful to the readers A5: Figure 6 was added to the Ms to explain the proposed mechanism R6. The authors have previously studied the protective effects of minocycline against UCB neurotoxicity -- minocycline is a known Ca chelator (whereas non Ca chelator minocycline derivatives do not show this neuroprotective property) -- would be of interest in the discussion to visit these effects. A6) We agree with the comment and we plan to test the direct effect of minocycline on UCB induced calcium oscillations in a near future. A paragraph dealing with the effects of minocycline on UCB neurotoxicity was added to the discussion. We hope to have comprehensively addressed the critiques raised by the reviewer and we look forward to the acceptance of the revised version. Cristina Bellarosa, PhD Corresponding author

Bilirubin disrupts calcium homeostasis in neonatal hippocampal neurons: A new pathway of neurotoxicity

Rossana Rauti [a 1]*, Mohammed Qaisiy [b2] , Claudio Tiribelli [b], Laura Ballerini [a], Cristina Bellarosa[b]*

Affiliations

a International School for Advanced Studies (SISSA), Via Bonomea, 265, 34136 Trieste, Italy

b Fondazione Italiana Fegato (FIF), Bldg Q - AREA Science Park Basovizza, SS14 Km 163,5, 34149 Trieste, Italy

1 Present Address: Department of Biomedical Engineering, Tel Aviv University, Tel Aviv, Israel

2 Present Address: College of Pharmacy and Medical Sciences, Hebron University, Hebron, West Bank, Palestine

* Corresponding authors:

Cristina Bellarosa (main corresponding author)

Bldg Q - AREA Science Park Basovizza
SS14 Km 163,5
34149 Trieste - Italy
Phone 040/375 7921
Fax 040/375 7832
email: cristina.bellarosa@fegato.it

Rossana Rauti

email: rrauti@sissa.it

Conflict of Interests

The authors report no conflicts of interest

Abstract

Severe hyperbilirubinemia leads to bilirubin encephalopathy in neonates, causing irreversible neurological sequelae. We investigated the nature of neuronal selective vulnerability to unconjugated bilirubin (UCB) toxicity. The maintenance of intracellular calcium homeostasis is crucial for neuron survival. Calcium release from endoplasmic reticulum (ER) during ER-stress can lead to apoptosis trough the activation of Caspase-12. By live calcium imaging we monitored the generation of calcium signals in dissociated hippocampal neurons and glial cells exposed to increasing UCB concentrations. We showed the ability of UCB to alter intracellular calcium homeostasis, inducing the appearance of repetitive intracellular calcium oscillations. The contribution of intracellular calcium stores and the induction and activation of proteins involved in the apoptotic calcium-dependent signaling were also assessed .Thapsigargin, a specific inhibitor of Sarco/endoplasmic reticulum ATPase (SERCA) pumps, significantly reduced the duration of Ca^{2+} oscillation associated with UCB exposure indicating that UCB strongly interfered with the reticulum calcium stores. On the contrary, in pure astrocyte cultures, spontaneous Ca^{2+} transient duration was not altered by UCB. The protein content of GRP78, AT6, CHOP, Calpain and Caspase-12 of neuronal cells treated with UCB for 24h was at least 2-fold higher compared to controls. Calcium-dependent Calpain and Caspase-12 induction by UCB were significantly reduced by 50% and 98% respectively when cells were pretreated with the ER-stress inhibitor 4-PBA.

These results show the strong and direct interference of UCB with neuronal intracellular Ca^{2+} dynamics, suggesting ER Ca^{2+} stores as a primary target of UCB toxicity with the activation of the apoptotic ER-stress-dependent pathway.

Keywords

Neuroscience; Kernicterus; Bilirubin neurotoxicity; Calcium imaging; ER Ca^{2+} stores; Apoptotic pathways

Introduction

Elevated level of unconjugated bilirubin (UCB) is responsible for the clinical manifestation of neonatal jaundice. When transient, this phenomenon has no clinical consequences, however prolonged and severe hyperbilirubinemia may lead to accumulation of bilirubin and encephalopathy or to a more severe condition named kernicterus (chronic bilirubin encephalopathy) characterized by irreversible neurological sequelae (1). This pigment circulates in blood bound to albumin (UCB) with only a minimal free fraction known as free bilirubin (Bf). When the plasma concentration bilirubin is markedly elevated, the Bf can passively cross cell membrane (2) with the central nervous system as the most vulnerable organ (3). Neurons, and in particular immature ones, are mostly sensitive to UCB toxicity (4,5).

Several studies showed the effects of UCB toward plasma membrane, mitochondria, endoplasmic reticulum (ER), calcium homeostasis, redox state and increased cell death by apoptosis (6). The ability of UCB to alter directly, at the molecular level, neuronal intracellular calcium homeostasis potentially triggering apoptosis in a cell autonomous manner has not been experimentally challenged. Besides calcium storage and signaling, a key function of the ER is the folding and processing of newly synthesized membrane and secretory proteins. Impairments of these functions are responsible of a pathological state termed ER stress that will induce apoptosis if ER functioning cannot be restored.

Among the different intracellular pathways involved in UCB neurotoxicity, in the last decade ER-stress was demonstrated to be a key mechanism both *in vitro* and *in vivo* (7–13). Whole genome gene expression analysis of SH-SY5Y cells exposed to UCB appears similar to the one obtained exposing cells to Thapsigargin which causes ER-stress by inhibiting the SERCA ATPase proteins that maintain the high calcium concentration in the ER(14). Although UCB accumulates in both neuronal and astrocyte cells, we have previously demonstrated, that UCB induces ER stress only in neuronal cells and not in astrocytes (15). Cytosolic increase of calcium was already described in different models of UCB neurotoxicity (16–18), however the underlying mechanisms remains partially unknown. In particular, the direct ability of UCB to selectively target neurons and neuronal spatial and temporal control of intracellular free calcium involving the ER storage machinery.

In this study we expose neonatal hippocampal neurons to UCB and monitor single cell and network activity by live calcium imaging. We documented the timing and appearance of intracellular calcium oscillations upon UCB exposure, such episodes are generated by each UCB treated neuron independently from the ongoing synaptic activity. We further show, by pharmacological

treatments, western blot and confocal microscopy that UCB induced ER-stress and calcium release from ER with subsequent Calpain accumulation and Caspase-12 activation. Of notice, these effects were not present in glial cells further confirming the different susceptibility to UCB of the two cell types.

Materials and Methods

Cell Culture Preparation

Isolation of primary hippocampal tissue was operated in agreement with the guidance of the National Institutes of Health and with the proper international and institutional standards for the care and use of animals in research (Italian Ministry of Health, in agreement with the EU Recommendation 2007/526/CE). All procedures were approved by the local veterinary authorities and performed in accordance with the Italian law (Decree 26/14) and the UE guidelines (2007/526/CE and 2010/63/UE). The animal use was approved by the Italian Ministry of Health. All efforts were made to reduce the number of animals used and to minimize animal suffering. All the reagents were purchased from Sigma-Aldrich if not otherwise indicated.

Dissociated hippocampal cultures were prepared from postnatal 2-3 days old (P2-P3) Wistar rats as previously reported (19,20).

Cells were plated on control poly-L-ornithine coated-glass coverslips and were incubated at 37 °C, 5 % CO_2 in a culture medium consisting of Neurobasal Medium (Gibco), supplemented with B27 (2%; Gibco), Glutamax (10 mM; Gibco), and Gentamycin (500×10^{-9} M; Gibco). Half of the culture medium was renewed four days after seeding. Cultures were grown until 8-10 days in vitro (DIV) and then used for experiments (21).

Primary glial cultures were isolated from neonatal rat (Wistar) cortices at postnatal day 2-3 (P2−P3), as previously described (22,23). Cells were dissociated and grown into plastic 150 cm^2 flasks and incubated at 37 °C; 5 % CO_2 in culture medium composed of DMEM (Invitrogen), supplemented with 10 % fetal bovine serum (FBS; Thermo Fisher), 100 IU/ mL penicillin, and 10 mg/mL streptomycin. After 3 weeks, glial cells were incubated for 5 minutes with a 10% trypsin/EDTA solution, detached from the flask and then plated on poly-L-ornithine (Sigma) coated coverslips (Kindler, EU) at a concentration of 50000 cells in a volume of 200 µL.

Treatments

UCB toxicity is related to the amount of the free bilirubin (Bf) (24) and the threshold value of toxicity in vitro occurs at Bf of 70 nM (25). Three different Bf concentration were tested: 40 nM, 90 nM and 140 nM. Bilirubin (Sigma Aldrich) was purified as previously described (26), dissolved in DMSO (3 µg/µL) and added to cell medium or to recording solution in the presence of BSA 30µM. The concentration of total bilirubin necessary to reach the desired Bf concentration (40 nM, 90 nM and 140 nM) in the presence of BSA 30 µM was calculated according to Roca et al.(27). Accordingly, control experiments were performed exposing the cells to an equal amount of DMSO. Phenylbutyric acid (4-PBA, Sigma Aldrich) was prepared by titrating equimolecular amount of 4-PBA with sodium hydroxide to pH 7.4. Cells were pre-treated with 2 mM of 4-PBA for 2 h and then treated with DMSO or UCB at the indicated Bf for additional 24 h in the presence of 4-PBA. Thapsigargin (Santa Cruz) and Carbonyl cyanide 3-chlorophenylhydrazone (Sigma Aldrich) were dissolved in DMSO. TTX (Latoxan) was dissolved in water (1 mM).

Live cell imaging

Neuronal and glial cells were incubated in 4 µM Oregon Green 488 BAPTA-1 AM (Invitrogen) for 40 min (37 °C; 5 % CO_2) (19,23). The samples were then placed in a recording chamber mounted on an inverted microscope (Nikon Eclipse Ti-U) where they were continuously perfused at RT by a recording solution of the following composition (mM): 150 NaCl, 4 KCl, 1 $MgCl_2$, 2 $CaCl_2$, 10 HEPES, 10 glucose (pH adjusted to 7.4 with NaOH). Ca^{2+}-free solution was identical to the recording solution except for (in mM): 0 CaCl2, 3 MgCl2, 5 EGTA.

Cultures were visualized with a 20 × objective (0.45 NA) and recordings were performed from visual fields (680 × 680 µm2, binning 4). Neuronal and glial cells positively stained by Ca2+dye Oregon green 488 BAPTA-1 were simultaneously visualized within the sampled area and on average 30 ± 10 fluorescent cells were measured in each field.

Ca^{2+}-dye was excited at 488 nm with a mercury lamp; excitation light was separated from the light emitted from the sample using a 395 nm dichroic mirror and ND filter (1/8). Images were continuously acquired (exposure time 150 ms) using an ORCA-Flash4.0 V2 sCMOS camera (Hamamatsu). The imaging system was controlled by an integrating imaging software (HCImage Live). All the drugs were diluted with recording solution at the following concentrations (in µM): 1 TTX, 2 carbonyl cyanide 3-chlorophenylhydrazone (CCCP), 5 thapsigargin.

Recorded images were analyzed off-line with Fiji (selecting ROIs around cell bodies), Clampfit software (pClamp suite, 10.2 version; Molecular Devices LLC, US) and Igor Pro Software (6.32 A version; WaveMetrics, Lake Oswego, Oregon, USA).

Intracellular Ca2+transients were expressed as fractional amplitude increase ($\Delta F/F_0$, where F0 is the baseline fluorescence level and ΔF is the rise over baseline); we determine the onset time of neuronal activation by detecting those events in the fluorescence signal that exceed at least five times the standard deviation of the noise. Oscillation duration was defined as the time from the beginning of the calcium rise over the baseline to the time when the amplitude declined to the baseline. Hence, after obtaining the average values from each cell in a visual field, data were pooled for all the samples recorded under the same experimental conditions and averaged for further comparison.

Western blot

Total proteins were extracted by lysing the cells in ice-cold cell lysis buffer (Cell Signaling Technology, USA). Protein concentration was determined by the bicinchoninic acid protein assay (BCA) according to manufacturer's instructions. Equal amounts of protein were separated by 12% SDS–polyacrylamide gel electrophoresis (SDS-PAGE) and transferred to PVDF membranes (Bio-Rad Laboratories). Membranes were blocked in 5 % milk or 4 % BSA in T-TBS (0.2 % Tween 20, 20 mM Tris–HCl (pH 7.5) and 500 mM NaCl) and incubated overnight at 4 °C with primary antibodies: anti GRP78 (Santa Cruz Biotechnology, sc-13968), anti ATF-6α (Santa Cruz Biotechnology, sc-166659), anti GADD153 (CHOP) (Gene Tex, GTX112827), anti Calpain (Santa Cruz Biotechnology, sc-30064), anti CASP12 (Elab Science, E-AB-64000), anti β-Tubulin (Santa Cruz Biotechnology, sc-32293)) and anti Actin (Sigma Aldrich, A 2066). Membranes were then incubated with anti-rabbit (Dacko Laboratories, Dako-p0448) or anti-mouse HRP-conjugated secondary antibody (Dacko Laboratories, Dako-p0260). Protein bands were detected by peroxide reaction using ECL Plus Western Blot detection system solutions (ECL Plus Western Blot detection reagents, GE-Healthcare Bio-Sciences). The relative intensities of protein bands were scanned and analyzed using the C-DiGit ® Blot Scanner - LI-COR (Biosciences),. The optical density of the the bands of interest were normalized to Actin or β-Tubulin and represented as relative to DMSO treated cells. Data are the mean ± SD of four independent experiments .

Immunocytochemistry

Cultured hippocampal neurons (2 cultures; 9-10 DIV) were incubated with Bf 90 nM for 24h. Cultures were then fixed by 4% formaldehyde in PBS for 20 min at RT and blocked and permeabilized in 5% fetal bovine serum (FBS), 0.3% Triton-X 100 in PBS for 30 min at RT. Samples were incubated with primary antibodies anti Calpain (Santa Cruz Biotechnology, sc-30064), 1:500 dilution; anti CASP12 (Elab Science, E-AB-64000),, 1: 250 dilution; anti-β-tubulin

III (Sigma,T2200), 1:500 dilution) diluted in PBS with 5% FBS for 45 min. Cultures were then incubated with secondary antibodies (Alexa 488 goat antimouse (Invitrogen, A32723), 1:500 dilution; Alexa 594 goat antirabbit (Invitrogen, A32740), 1:500 dilution) and DAPI to stain the nuclei for 45 min at RT and finally mounted on 1 mm thick glass coverslips using the Fluoromont mounting medium (Sigma). Images were acquired using a Nikon C2 Confocal, equipped with Ar/Kr, He/Ne, and UV lasers. Images were acquired with a 20× (.. NA) and 40× (..NA) objective. Confocal sections were acquired every 0.5 µm and identical binning, gains, and exposure times were used for all images of the same marker. Image analysis was performed using Volocity software (Volocity 3D image analysis software, PerkinElmer, USA). Each Z-stack was collapsed into a maximum intensity projection image, prior to intensity analysis. For fluorescence intensity analysis of caspase 12 and Calpain, a mask was created enclosing the entire neuron. The threshold for creating the mask was determined based on average and SD values for every image (28).

Statistical Analysis

All data are presented as mean ± standard deviation (S.D.) of the mean. A statistically significant difference between two data sets was assessed by Student's t-test for parametric data. Differences between different groups were assessed using two-way ANOVA and multiple comparisons, adjusted by Bonferroni or Holm-Sidak correction. Statistical significance was determined at $P < 0.05$, unless otherwise indicated. Significance was graphically indicated as follows: *$P < 0.05$, **$P < 0.01$, ***$P < 0.001$.

Results

1. UCB affects Ca^{2+} transients

To investigate the ability of UCB to impact neuronal calcium dynamics in functional networks, dissociated hippocampal neurons were treated with different concentrations of free bilirubin (see methods) and the emerging effect was explored by live calcium imaging.

Neurons, stained with the membrane permeable Ca^{2+} dye Oregon Green 488 BAPTA-1 AM, were simultaneously visualized within the sampled area (visual field 680 × 680 μm^2, Figure 1A, left panel); an of average 30 ± 4 fluorescent cells were isolated and imaged in each visual field. Calcium

activity was assessed before and after bilirubin exposure. Calcium dynamics did not differ in saline solution among the different samples, that were pooled together and collectively named Control.

In Figure 1A (right panel) sample tracings of spontaneous fluorescent recordings (left traces) or bilirubin-induced (right traces) at the three different concentrations (40 nM, 90 nM, and 140 nM Bf) respectively. UCB significantly (** $p < 0.01$) increased the duration of Ca^{2+} waves (42 ± 6 s, n = 150 cells, Bf 40 nM; 54 ± 8 s, n = 140 cells, Bf 90 nM; 50 ± 8 s, n = 155 cells, Bf 140 nM; n = 5 samples for each condition from 3 different series of cultures) when compared to controls (7 ± 3 s, n = 450 cells, n = 15 samples, from 3 different series of cultures; see the histogram plot in Figure 1A, bottom panel). Bilirubin-induced Ca dynamics are reversible. 5 min washout did not affected the Ca++ dynamics brought about by 10 min bilirubin application, for all concentrations tested (Bf 40 nM: from 42 ± 6 s to 37 ± 10 s, after 5 min removal, n = 5 cells; Bf 90 nM: from 54 ± 8 s to 51 ± 8 s, after 5 min removal, n= 5 cells; Bf 140 nM: from 50 ± 6 s to 42 ± 8 s, after 5 min removal, n= 4 cells). Conversely, upon 10 min bilirubin washout, a decrease in the Ca++ events' duration was detected (Bf 40 nM: 11 ± 10 s, n = 5 cells; Bf 90 nM: 22 ± 8 s, n = 5 cells; Bf 140 nM: 27 ± 8 s, n= 5 cells), suggestive of a progressive clearance of bilirubin, with the Ca++ event duration resembling that of controls (See supplementary Fig 1S).

Since we detected similar effects of the three different UCB concentrations, in the next set of experiments we selected 90 nM Bf as the concentration for subsequent experiments. Hippocampal cultured neurons once reorganized ex vivo develop functional synaptic circuits characterized by the generation of electrical activity. We next investigated whether the effect of UCB in changing calcium oscillations depended on the generation and propagation of action potentials. Fig 1B shows that application (≥ 5 min) of Tetrodotoxin (TTX, 1 μM; a blocker of fast voltage-dependent Na^+ channels) fully blocked the spontaneous bursts of activity (middle trace) but did not block the calcium oscillations induced by UCB application, as this treatment had only a slight effect on the duration of the Ca^{2+} oscillations, significantly (** $p < 0.01$) higher when compared before (8 ± 3 s, n = 120 cells, n = 4 samples, from 2 different series of cultures) and after (44 ± 10 s, n = 120 cells, n = 4 samples, from 2 different series of cultures) UCB perfusion.

These results point to the ability of UCB to impact calcium pathways although do not allow to distinguish whether the effect is at the extracellular or intracellular level.

2. Intracellular calcium dependence of UCB calcium signals.

In order to explore the nature of the observed oscillatory pattern induced by UCB, we investigated its dependence on extracellular and intracellular calcium. As shown in Figure 2A, when cultures were superfused with a calcium-free solution, these events showed only a slight, not significant, reduction in their duration when compared to UCB application (40 ± 8 vs. 50 ± 10 s, n = 120 cells, n = 4 samples from 2 series of cultures) but a significant (** $p < 0.01$) increase when compared to the control (8 ± 3 s, n = 120 cells, n = 4 samples from 2 series of cultures). Remarkably, the impact of UCB on calcium oscillations is not dependent on the absence of external calcium.

We then explored the possible contribution of intracellular Ca^{2+} sources, starting from the role of mitochondrial Ca^{2+} uptake by the use of mitochondrial protonophore carbonyl cyanide 3-chlorophenylhydrazone (CCCP) which dissipates the proton gradient across the inner mitochondrial membrane and disrupts Ca^{2+} uptake (29).

Figure 2B shows that CCCP treatment (2 µM; 3-7 min) caused a slight, not significant reduction (in the Ca^{2+} oscillations induced by UCB application (38 ± 6 vs. 44 ± 6 s, n = 120 cells, n = 4 samples from 2 series of cultures). Conversely, their duration was significantly (** $p < 0.01$) higher compared to the control condition (10 ± 2 s, n = 120 cells, n = 4 samples from 2 series of cultures). Another source of calcium store and release derives from the endoplasmic reticulum (ER). Thapsigargin (5 µM; 10 min), a specific inhibitor of sarco/endoplasmic reticulum ATPase (SERCA) pumps, greatly affected the ability of UCB to impact neuronal Ca^{2+} activity (Figure 2C) by reducing the duration of Ca^{2+} oscillation induced by UCB (16 ± 4 *vs* 51 ± 8 s, respectively, $p < 0.01$, n = 110 cells, n = 4 samples from 2 series of cultures).

3. UCB does not impact on Ca^{2+} transients in glial cells.

To investigate if UCB has exclusively the ability to impair neuronal network, pure glial cells cultures were grown for 3 weeks and calcium imaging recordings were performed with or without UCB, at the three different concentrations. Figure 3A, left-panel, shows a representative visual field of glial cells loaded with the Ca^{2+} permeable dye and on the left panel, representative fluorescent tracings of glial cells before and after UCB perfusion, at the three different concentrations. Contrary to what observed in neurons, UCB at the 3 concentrations tested has no effect on Ca^{2+} oscillation durations comparing control cultures (Figure 3B). Surprisingly, UCB has no impact on Ca^{2+} oscillation durations comparing control cultures (18 ± 4s, n = 60 cells, n = 2 samples from 2 series of cultures), with Bf 40 nM (24 ± 5s, n = 58 cells, n = 2 samples from 2 series of cultures), Bf 90nM(18 ± 6s, n = 60 cells, n = 2 samples from 2 series of cultures), andBf 140nM(22 ± 6s, n = 58 cells, n = 2 samples from 2 series of cultures; see plot in Figure 3B).

4. UCB induces the expression of proteins involved in calcium-dependent apoptotic signaling

ER function as a dynamic Ca^{+2} store and has a very high Ca^{+2} level compared to cytosol. When ER calcium stores are depleted, the unfolded protein response (UPR) is activated and when prolonged, it leads to apoptosis. We analyzed the protein expression of ER stress-related genes and of the proteins involved in calcium-dependent apoptotic signaling in the neuronal cells exposed to Bf 90 nM for 24 h. Compared to DMSO-treated cells, neuronal cells treated with UCB showed an induction of GRP78 (1.9 ± 0.8 folds, $p < 0.05$), cleaved p50 ATF6 (2.1 ± 0.9 folds, $p < 0.05$) and CHOP (2.7 ± 1.4 folds, $p < 0.01$). Neuronal cells treated with UCB showed also an up-regulation of Calpain (1.95 ± 0.9 folds, $p < 0.05$) and the activation of the cleaved Caspase-12 (5.4 ± 1.5 folds, $p < 0.01$) (Figure 4 A-B).

Caspase-12 and Calpain activation were also investigated in neuronal cultures treated with UCB Bf 90 nM for 24h, by immunofluorescence staining, co-immunolabeling the cytoskeletal neuronal component β-tubulin III (Figure 5). UCB induced a significant (** $p < 0.01$ increase in Caspase 12 intensity ((176 ± 20%, n = 7 visual fields, from 2 series of cultures),) compared to control sister cultures (n = 7 visual fields, from 2 series of cultures; see bar plot in Figure 5A). Similarly, Bf 90 nM promoted a significant (** $p < 0.01$; ; n = 7 visual fields, from 2 series of cultures, Figure 5B) increase in Calpain intensity (216 ± 25%; n = 7 visual fields, from 2 series of cultures) compared to control sister cultures (see bar plot in Figure 5B).

5. ER stress inhibition reduces Calpain and Cleaved Caspase-12 induction by UCB

A severe and prolonged ER-stress causes cell death. To study the effect of ER-stress on the activation of calcium-dependent Calpain/Caspase-12 signaling, cells were treated with UCB in the presence of 4-PBA, a pharmacological chaperone promoting ER folding/trafficking, commonly considered as an ER-stress inhibitor. Compared to cells treated with Bf 90 nM in the absence of 4-PBA, the presence of 4-PBA showed a 55% (*$p < 0.05$) and 97% (**$p < 0.001$) down-regulation in the induction of Calpain and cleaved Caspase-12, respectively (Figure 4 C-D).

Discussion

The exposure of neurons to UCB *in vitro* is associated with the perturbation of intracellular calcium homeostasis (16–18) and increased death by apoptosis (1). UCB damage seems to affect several vital functions rather than a single cell death pathway (30) and UCB induced cell death is not linked to a single pathway. In addition to the role of mitochondria in mediating apoptotic cell death initiated by UCB (31), the activation of caspase 8, an initiator of apoptosis, was described (32) as

the participation of NMDA receptors, along with the bilirubin-induced inhibition of protein kinase C activity (33).

Here we investigated the ability of UCB to activate the cell signaling that leads to apoptosis starting from ER-stress, involving ER calcium release, Calpain increase and Caspase-12 activation (7). For the first time, the impact of bilirubin in neuronal cultures was assessed by taking advantage of the live-cell calcium technique, an important tool able to provide highly qualitative and quantitative information regarding intracellular mechanisms involving calcium signaling (34).

The main finding is the novel demonstration that bilirubin has the ability to strongly impact the complex pattern of Ca^{2+} signaling in neuronal cultures. Dissociated hippocampal cultures allow direct experimental access to nervous microcircuits. This preparation has been used in neuroscience research for a long time(23,35) and represents a useful model for studying the dynamics of brain neurotoxicity(36,37). Our study shows that the application of bilirubin results into larger repetitive Ca^{2+} oscillations, whose generation and spreading do not depend on action potential and thus synaptic activity (29) (Fig.1). Calcium is a key player of cell fate and regulates the activity of several proteins. Cells regulate the intracellular calcium through integrated channels located on plasma membrane, mitochondria and ER. We observed that blocking Ca^{2+} reuptake at the level of ER consistently suppressed oscillations led by UCB and suggested that UCB operate on the endoplasmic reticulum calcium sources (Fig.2). The ER plays a central role in cellular calcium storage, signaling and in the folding and processing of newly synthesized membrane and secretory protein. These calcium-dependent processes require high calcium activity for correct functioning (38). When ER calcium stores are depleted, the unfolded protein response (UPR) is activated initially to reestablish normal ER function. When the stress is severe and prolonged, ER-stress induces cell death (39). Under ER stress the genetic program activated involves both genes like grp78 that make cells resistant to the stressful conditions (40) and genes like gadd153 (CHOP) a major player in ER stress-induced apoptosis (41). ER-resident Caspase-12 is also involved in the execution of ER stress-induced apoptosis (42). Calpains, a family of Ca^{2+}-dependent cysteine proteases, have been shown to play a role in Caspase-12 activation (43) and elevation of cytoplasmic Ca^{2+} level leads to the accumulation and activation of Calpain at the ER membrane, where it can activate Caspase-12 (7).

The evidence that UCB operates on the endoplasmic reticulum calcium sources (Fig. 2) explains well the early ER-stress induction by UCB we have previously observed on SH-SY5Y (8,15). In the present work, we confirmed further the UPR activation by UCB, since we detected protein induction of the ER- resident chaperone GRP78/Bip and of the pro-apoptotic mediator CHOP (44)

after exposure of hippocampal neurons to UCB (Fig. 4 A-B). The increase in Ca^{+2} concentration in the cytosol activates Calpain, which cleaves and activates pro Caspase-12. Activated CASPASE 12 cleaves and activates downstream CASPASES 9 and 3 leading to apoptosis (7). UCB exposure on hippocampal neurons activates Calpain and Caspase-12 (Fig. 4A-B and 5) and this effect is blunted by 4-PBA (Fig. 4 C-D) indicating that this the activation of the apoptotic pathway is mediated by ER-stress induced by UCB.

Of notice is the observation that in astrocytes, the spontaneous glial Ca^{2+} transients duration was not altered by UCB (Fig. 3). This is in line with our previous demonstration that ER-stress does not occur in U87 astrocytoma cell line despite a intracellular UCB accumulation similar to neuronal cells (15). This finding may be at the basis of the higher sensitivity of neuronal than glial cells to UCB toxicity (4,5).

Increase intracellular Ca^{+2} events can be both an inducer of ER stress or/and a result of ER-stress. Further studied are needed to understand if UCB acts first directly on ER- membrane Ca^{2+} receptors causing Ca^{2+} release or if induces ER-stress. If ER-stress would be the primary event, the CHOP activation by UCB could be responsible for the Ca^{+2} depletion from ER. CHOP is a pro-apoptotic mediator of ER-stress induced ER oxidase 1α (ERO1α) activates the inositol-1,4,5-trisphosphate receptor (IP_3 R), leading to calcium release from ER (44). The release of Ca^{+2} form ER lumen can contribute significantly to cell death via Calpain/Caspase-12 (45,46). This hypothesis is sustained also from data collected on glial cells, where CHOP induction and intracellular calcium increase are both absent upon UCB treatment.

The strong and direct interference of UCB with neuronal intracellular Ca2+ dynamics can also explain the mechanisms involved in minocycline protection against bilirubin neurotoxicity. Minocycline is a broad-spectrum tetracycline antibiotic and in rat liver minocycline was demonstrated to be a Calcium ions chelator (47). In the hyperbilirubinemic Gunn Rat model, minocycline administration was demonstrated to prevent cerebellar hypoplasia (48), bilirubin-induced neurologic dysfunction (BIND) (49) and brainstem auditory evoked potentials (BAEPs) abnormalities (50) (51). Further investigation are needed to clarify minocycline mechanisms of action.

Conclusions

We have shown a strong and direct interference of UCB with neuronal intracellular Ca^{2+} dynamics, while the calcium homeostasis in glial cells remained undisturbed. Our data suggest the neuronal endoplasmic reticulum but not mitochondrial Ca^{2+} stores as a primary target of UCB. This induces the expression of ER-stress related proteins and the activation of the cytosolic calcium-dependent apoptosis pathway (Figure 6). These results may be relevant to understand the early events and a better treatment of bilirubin-induced neurological damage and to prevent the permanent neurological damages caused by kernicterus.

Acknowledgments

We thank FIF technician Sandra Leal for the purification of the amount of bilirubin needed to perform calcium imaging experiments. This work was supported in part by an intramural grant of Fondazione Italiana Fegato and by Taawon "Zamala Program" (Mohammed Qaisiya fellowship).

Conflict of Interests

The authors report no conflicts of interest

References

1. Watchko JF, Tiribelli C. Bilirubin-induced neurologic damage--mechanisms and management approaches. N Engl J Med. 21 novembre 2013;369(21):2021–30.

2. Zucker SD, Goessling W, Hoppin AG. Unconjugated bilirubin exhibits spontaneous diffusion through model lipid bilayers and native hepatocyte membranes. J Biol Chem. 16 aprile 1999;274(16):10852–62.

3. Gazzin S, Zelenka J, Zdrahalova L, Konickova R, Zabetta CC, Giraudi PJ, et al. Bilirubin accumulation and Cyp mRNA expression in selected brain regions of jaundiced Gunn rat pups. Pediatr Res. giugno 2012;71(6):653–60.

4. Falcão AS, Fernandes A, Brito MA, Silva RFM, Brites D. Bilirubin-induced immunostimulant effects and toxicity vary with neural cell type and maturation state. Acta Neuropathol (Berl). luglio 2006;112(1):95–105.

5. Brito MA, Rosa AI, Falcão AS, Fernandes A, Silva RFM, Butterfield DA, et al. Unconjugated bilirubin differentially affects the redox status of neuronal and astroglial cells. Neurobiol Dis. gennaio 2008;29(1):30–40.

6. Watchko JF. Kernicterus and the molecular mechanisms of bilirubin-induced CNS injury in newborns. Neuromolecular Med. 2006;8(4):513–29.

7. Lai E, Teodoro T, Volchuk A. Endoplasmic reticulum stress: signaling the unfolded protein response. Physiol Bethesda Md. giugno 2007;22:193–201.

8. Calligaris R, Bellarosa C, Foti R, Roncaglia P, Giraudi P, Krmac H, et al. A transcriptome analysis identifies molecular effectors of unconjugated bilirubin in human neuroblastoma SH-SY5Y cells. BMC Genomics. 2009;10:543.

9. Oakes GH, Bend JR. Global changes in gene regulation demonstrate that unconjugated bilirubin is able to upregulate and activate select components of the endoplasmic reticulum stress response pathway. J Biochem Mol Toxicol. aprile 2010;24(2):73–88.

10. Barateiro A, Vaz AR, Silva SL, Fernandes A, Brites D. ER stress, mitochondrial dysfunction and calpain/JNK activation are involved in oligodendrocyte precursor cell death by unconjugated bilirubin. Neuromolecular Med. dicembre 2012;14(4):285–302.

11. Qaisiya M, Coda Zabetta CD, Bellarosa C, Tiribelli C. Bilirubin mediated oxidative stress involves antioxidant response activation via Nrf2 pathway. Cell Signal. marzo 2014;26(3):512–20.

12. Vodret S, Bortolussi G, Jašprová J, Vitek L, Muro AF. Inflammatory signature of cerebellar neurodegeneration during neonatal hyperbilirubinemia in Ugt1 (-/-) mouse model. J Neuroinflammation. 24 marzo 2017;14(1):64.

13. Vodret S, Bortolussi G, Iaconcig A, Martinelli E, Tiribelli C, Muro AF. Attenuation of neuro-inflammation improves survival and neurodegeneration in a mouse model of severe neonatal hyperbilirubinemia. Brain Behav Immun. 2018;70:166–78.

14. Schiavon E, Smalley JL, Newton S, Greig NH, Forsythe ID. Neuroinflammation and ER-stress are key mechanisms of acute bilirubin toxicity and hearing loss in a mouse model. PloS One. 2018;13(8):e0201022.

15. Qaisiya M, Brischetto C, Jašprová J, Vitek L, Tiribelli C, Bellarosa C. Bilirubin-induced ER stress contributes to the inflammatory response and apoptosis in neuronal cells. Arch Toxicol. aprile 2017;91(4):1847–58.

16. Brito MA, Brites D, Butterfield DA. A link between hyperbilirubinemia, oxidative stress and injury to neocortical synaptosomes. Brain Res. 5 novembre 2004;1026(1):33–43.

17. Zhang B, Yang X, Gao X. Taurine protects against bilirubin-induced neurotoxicity in vitro. Brain Res. 12 marzo 2010;1320:159–67.

18. Liang M, Yin X-L, Shi H-B, Li C-Y, Li X-Y, Song N-Y, et al. Bilirubin augments Ca2+ load of developing bushy neurons by targeting specific subtype of voltage-gated calcium channels. Sci Rep [Internet]. 27 marzo 2017 [citato 16 ottobre 2018];7. Available at: https://www.ncbi.nlm.nih.gov/pmc/articles/PMC5427978/

19. Bosi S, Rauti R, Laishram J, Turco A, Lonardoni D, Nieus T, et al. From 2D to 3D: novel nanostructured scaffolds to investigate signalling in reconstructed neuronal networks. Sci Rep. 24 aprile 2015;5:9562.

20. Rauti R, Medelin M, Newman L, Vranic S, Reina G, Bianco A, et al. Graphene Oxide Flakes Tune Excitatory Neurotransmission in Vivo by Targeting Hippocampal Synapses. Nano Lett. 08 2019;19(5):2858–70.

21. Pampaloni NP, Lottner M, Giugliano M, Matruglio A, D'Amico F, Prato M, et al. Single-layer graphene modulates neuronal communication and augments membrane ion currents. Nat Nanotechnol. 2018;13(8):755–64.

22. Calegari F, Coco S, Taverna E, Bassetti M, Verderio C, Corradi N, et al. A regulated secretory pathway in cultured hippocampal astrocytes. J Biol Chem. 6 agosto 1999;274(32):22539–47.

23. Rauti R, Lozano N, León V, Scaini D, Musto M, Rago I, et al. Graphene Oxide Nanosheets Reshape Synaptic Function in Cultured Brain Networks. ACS Nano. 26 2016;10(4):4459–71.

24. Ahlfors CE, Wennberg RP, Ostrow JD, Tiribelli C. Unbound (free) bilirubin: improving the paradigm for evaluating neonatal jaundice. Clin Chem. luglio 2009;55(7):1288–99.

25. Ostrow JD, Pascolo L, Tiribelli C. Reassessment of the unbound concentrations of unconjugated bilirubin in relation to neurotoxicity in vitro. Pediatr Res. dicembre 2003;54(6):926.

26. McDonagh AF, Assisi F. The ready isomerization of bilirubin IX- in aqueous solution. Biochem J. settembre 1972;129(3):797–800.

27. Roca L, Calligaris S, Wennberg RP, Ahlfors CE, Malik SG, Ostrow JD, et al. Factors affecting the binding of bilirubin to serum albumins: validation and application of the peroxidase method. Pediatr Res. dicembre 2006;60(6):724–8.

28. Ahmad F, Das D, Kommaddi RP, Diwakar L, Gowaikar R, Rupanagudi KV, et al. Isoform-specific hyperactivation of calpain-2 occurs presymptomatically at the synapse in Alzheimer's disease mice and correlates with memory deficits in human subjects. Sci Rep. 3 settembre 2018;8(1):13119.

29. Fabbro A, Pastore B, Nistri A, Ballerini L. Activity-independent intracellular Ca2+ oscillations are spontaneously generated by ventral spinal neurons during development in vitro. Cell Calcium. aprile 2007;41(4):317–29.

30. Ostrow JD, Pascolo L, Brites D, Tiribelli C. Molecular basis of bilirubin-induced neurotoxicity. Trends Mol Med. febbraio 2004;10(2):65–70.

31. Rodrigues CMP, Solá S, Brites D. Bilirubin induces apoptosis via the mitochondrial pathway in developing rat brain neurons. Hepatol Baltim Md. maggio 2002;35(5):1186–95.

32. Seubert JM, Darmon AJ, El-Kadi AOS, D'Souza SJA, Bend JR. Apoptosis in murine hepatoma hepa 1c1c7 wild-type, C12, and C4 cells mediated by bilirubin. Mol Pharmacol. agosto 2002;62(2):257–64.

33. Grojean S, Koziel V, Vert P, Daval JL. Bilirubin induces apoptosis via activation of NMDA receptors in developing rat brain neurons. Exp Neurol. dicembre 2000;166(2):334–41.

34. Grienberger C, Konnerth A. Imaging calcium in neurons. Neuron. 8 marzo 2012;73(5):862–85.

35. Lovat V, Pantarotto D, Lagostena L, Cacciari B, Grandolfo M, Righi M, et al. Carbon nanotube substrates boost neuronal electrical signaling. Nano Lett. giugno 2005;5(6):1107–10.

36. Shah PT, Yoon KW, Xu XM, Broder LD. Apoptosis mediates cell death following traumatic injury in rat hippocampal neurons. Neuroscience. agosto 1997;79(4):999–1004.

37. Silva RFM, Falcão AS, Fernandes A, Gordo AC, Brito MA, Brites D. Dissociated primary nerve cell cultures as models for assessment of neurotoxicity. Toxicol Lett. 5 maggio 2006;163(1):1–9.

38. Verkhratsky A. Physiology and pathophysiology of the calcium store in the endoplasmic reticulum of neurons. Physiol Rev. gennaio 2005;85(1):201–79.

39. Mekahli D, Bultynck G, Parys JB, De Smedt H, Missiaen L. Endoplasmic-reticulum calcium depletion and disease. Cold Spring Harb Perspect Biol. 1 giugno 2011;3(6).

40. Kaufman RJ. Stress signaling from the lumen of the endoplasmic reticulum: coordination of gene transcriptional and translational controls. Genes Dev. 15 maggio 1999;13(10):1211–33.

41. Oyadomari S, Mori M. Roles of CHOP/GADD153 in endoplasmic reticulum stress. Cell Death Differ. aprile 2004;11(4):381–9.

42. Nakagawa T, Zhu H, Morishima N, Li E, Xu J, Yankner BA, et al. Caspase-12 mediates endoplasmic-reticulum-specific apoptosis and cytotoxicity by amyloid-beta. Nature. 6 gennaio 2000;403(6765):98–103.

43. Nakagawa T, Yuan J. Cross-talk between two cysteine protease families. Activation of caspase-12 by calpain in apoptosis. J Cell Biol. 21 agosto 2000;150(4):887–94.

44. Li G, Mongillo M, Chin K-T, Harding H, Ron D, Marks AR, et al. Role of ERO1-alpha-mediated stimulation of inositol 1,4,5-triphosphate receptor activity in endoplasmic reticulum stress-induced apoptosis. J Cell Biol. 21 settembre 2009;186(6):783–92.

45. Manié SN, Lebeau J, Chevet E. Cellular mechanisms of endoplasmic reticulum stress signaling in health and disease. 3. Orchestrating the unfolded protein response in oncogenesis: an update. Am J Physiol Cell Physiol. 15 novembre 2014;307(10):C901-907.

46. Lai E, Teodoro T, Volchuk A. Endoplasmic reticulum stress: signaling the unfolded protein response. Physiol Bethesda Md. giugno 2007;22:193–201.

47. Antonenko YN, Rokitskaya TI, Cooper AJL, Krasnikov BF. Minocycline chelates Ca2+, binds to membranes, and depolarizes mitochondria by formation of Ca2+-dependent ion channels. J Bioenerg Biomembr. aprile 2010;42(2):151–63.

48. Lin S, Wei X, Bales KR, Paul ABC, Ma Z, Yan G, et al. Minocycline blocks bilirubin neurotoxicity and prevents hyperbilirubinemia-induced cerebellar hypoplasia in the Gunn rat. Eur J Neurosci. luglio 2005;22(1):21–7.

49. Daood MJ, Hoyson M, Watchko JF. Lipid peroxidation is not the primary mechanism of bilirubin-induced neurologic dysfunction in jaundiced Gunn rat pups. Pediatr Res. novembre 2012;72(5):455–9.

50. Geiger AS, Rice AC, Shapiro SM. Minocycline blocks acute bilirubin-induced neurological dysfunction in jaundiced Gunn rats. Neonatology. 2007;92(4):219–26.

51. Rice AC, Chiou VL, Zuckoff SB, Shapiro SM. Profile of minocycline neuroprotection in bilirubin-induced auditory system dysfunction. Brain Res. 12 gennaio 2011;1368:290–8.

Figure Legends

Figure 1. UCB impact on Ca^{2+} signaling in hippocampal neuronal cultures.

(A) Snapshot of representative filed of neuronal cultures stained with the Oregon Green 488-Bapta-1 AM calcium indicator; repetitive Ca^{2+} events spontaneously (left) or UCB- induced (right) at the three different concentrations, recorded in hippocampal cultures; histogram of the average of Ca^{2+} oscillation duration in normal saline solution and id UCB Bf 40 nM, 90 nM and 140 nM, respectively (** $p < 0.01$; multiple comparisons two-way ANOVA test). (B) Repetitive Ca^{2+} fluorescence recordings in saline solution, TTX (1 μM) and in the presence of UCB Bf 90 nM; histogram reporting the duration of Ca^{2+} in the three different conditions (** $p < 0.01$; multiple comparisons two-way ANOVA test).

Figure 2. UCB effect on intracellular Ca^{2+} sources

(A) Repetitive Ca^{2+} fluorescence recordings in saline solution, 90 nM Bf, and in the absence of extracellular calcium; histogram reporting the duration of Ca^{2+} in the three different conditions (** $p < 0.01$; multiple comparisons two-way ANOVA test). (B) Repetitive Ca^{2+} fluorescence recordings in saline solution, 90 nM Bf, and in the presence of CCCP (2 μM); histogram reporting the duration of Ca^{2+} in the three different conditions (** $p < 0.01$; multiple comparisons two-way ANOVA test). (C) Repetitive Ca^{2+} fluorescence recordings in saline solution, 90 nM Bf, and in the presence of Thapsigargin (5 μM); histogram reporting the duration of Ca^{2+} in the three different conditions (** $p < 0.01$; multiple comparisons two-way ANOVA test).

Figure 3. UCB doesn't impact on Ca^{2+} signaling in glial hippocampal cultures.

(A) Snapshot of representative filed of glial cultures stained with the Oregon Green 488-Bapta-1 AM calcium indicator; repetitive Ca^{2+} events spontaneously (left) or UCB- induced (right) at the three different concentrations, recorded in hippocampal glial cultures; histogram of the average of Ca^{2+} oscillation duration in normal saline solution and id UCB Bf 40 nM, 90 nM and 140 nM, respectively.

Figure 4.. Effect of UCB treatment on proteins involved in calcium dependent apoptotic signaling in the presence or absence of ER stress inhibitor (4-PBA)

(A) Representative Western Blot for of GRP78, ATF6, CHOP, Calpain and cleaved Caspase-12 in neuronal cells treated with 0.3 % DMSO and Bf 90 nM for 24h. (B) The optical density of each band was normalized to Actin or β-Tubulin and represented as relative to cells treated with DMSO. (C) Representative Western Blot for Calpain and Cleaved Caspase-12 in neuronal cells exposed to 0.3 % DMSO or 90 nM Bf for 24 h in the presence (+) or absence (−) of 4-PBA. (D) The optical density of the the bands of Calpain and cleaved Caspase-12 were normalized to Actin or β-Tubulin and represented as relative to DMSO treated cells. Data are the mean ± SD of at least three independent experiments (*$P < 0.05$, **$P < 0.01$; Student t test)

Figure 5. Caspase-12 and Calpain expression induced by UCB

(A) Confocal microscopic images of two representative fields of hippocampal neuronal cultures grown on control (top) or incubated with UCB 90 nM Bf (bottom). Cells were immune-stained for β-tubulin III to point out neurons (in green, left columns), DAPI for nuclei (in blue, left columns), and Caspase-12 (in red, central columns), and Overlapping of all the three stains (right columns). The percentage of Caspase-12 intensity in the two conditions was evaluated and represented as histogram (** $p < 0.01$; Student t test). (B) Confocal microscopic images of two representative

fields of hippocampal neuronal cultures grown on control (top) or incubated with UCB 90 nM Bf (bottom). Cells were immune-stained for β-tubulin III (in green, left columns), DAPI for nuclei (in blue, left columns), and Calpain (in red, central columns), and Overlapping of all the three stains (right columns). The percentage of Calpain intensity in the two conditions was evaluated and represented as histogram (** $p < 0.01$; Student t test).

Figure 6. Proposed pathophysiology of UCB on neuronal cell calcium dynamics and downstream effects

Our data suggest the neuronal endoplasmic reticulum Ca^{2+} stores as a primary target of UCB. This induces the expression of ER-stress related proteins and the activation of the cytosolic calcium-dependent apoptosis pathway involving Calpain induction and Caspase 12 activation.

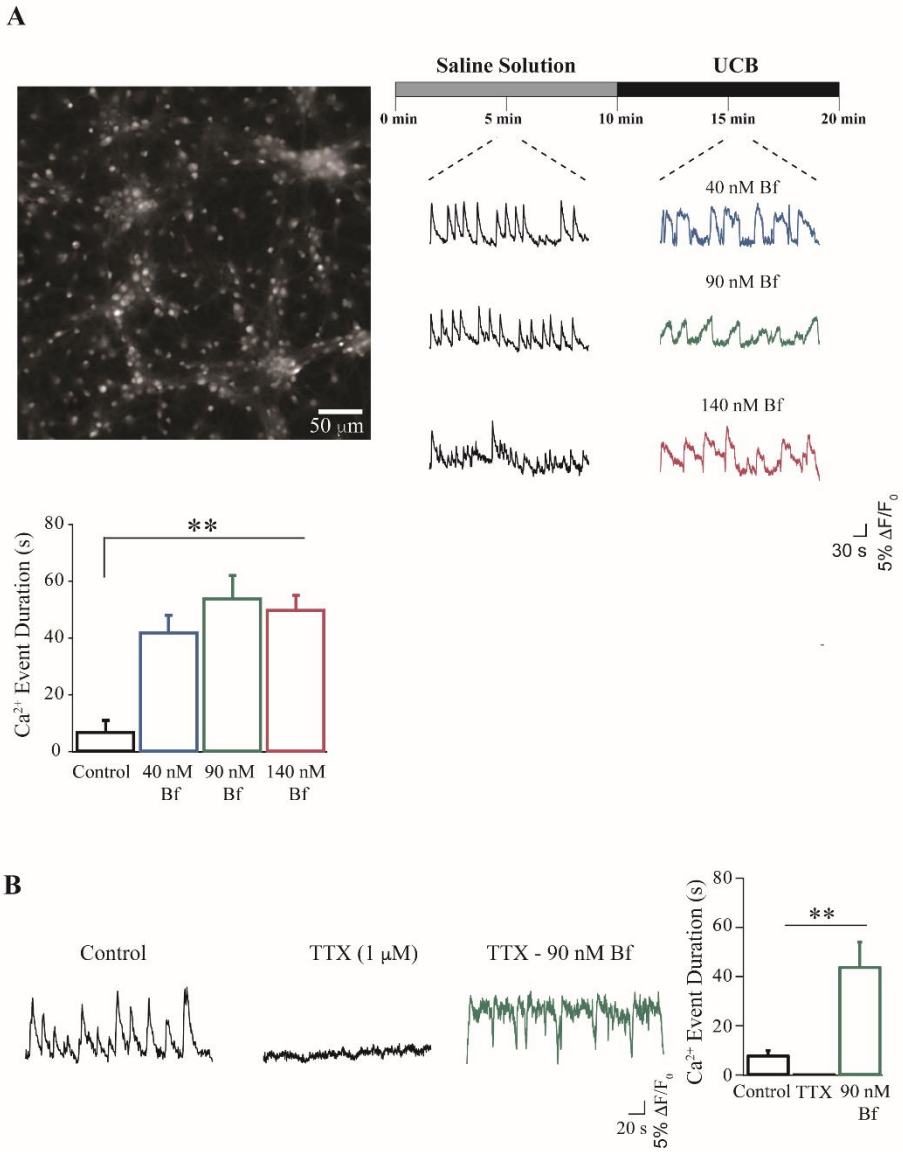
A
Saline Solution
UCB
0 min
5 min
10 min
15 min
20 min
40 nM Bf
90 nM Bf
140 nM Bf
50 μm
30 s
5% ΔF/F0
Ca2+ Event Duration (s)
**
Control
40 nM Bf
90 nM Bf
140 nM Bf
B
Control
TTX (1 μM)
TTX - 90 nM Bf
20 s
5% ΔF/F0
Ca2+ Event Duration (s)
**
Control
TTX
90 nM Bf

591

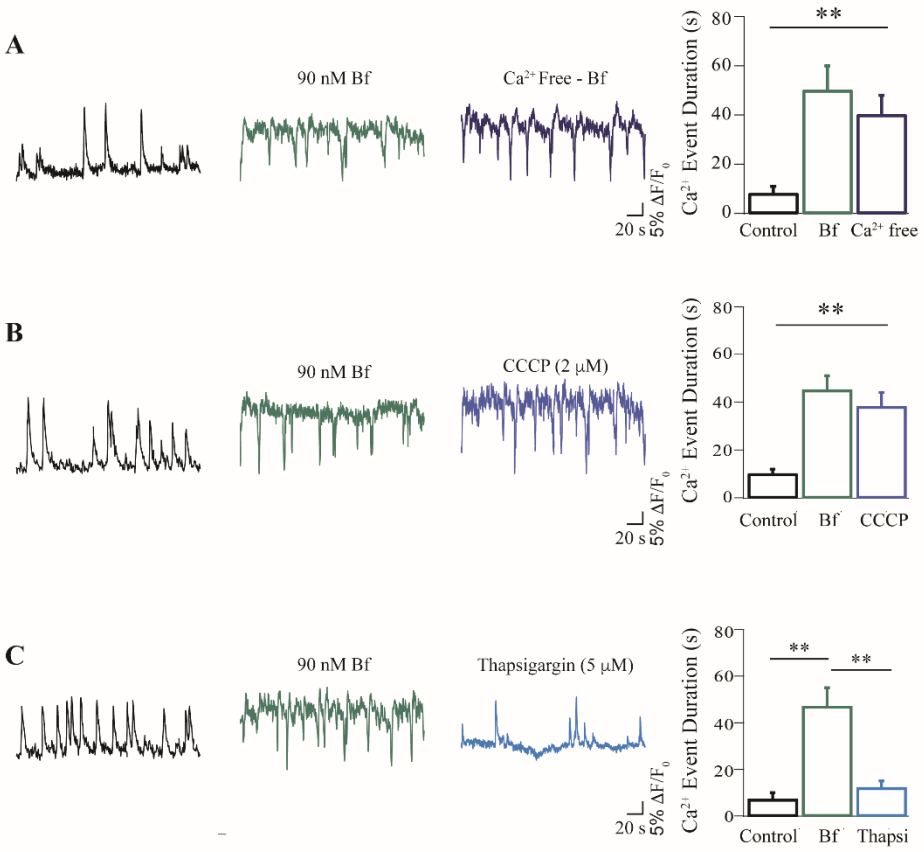
A
90 nM Bf
Ca2+ Free - Bf
20 s
5% ΔF/F0
Ca2+ Event Duration (s)
80
60
40
20
0
**
Control
Bf
Ca2+ free
B
90 nM Bf
CCCP (2 μM)
20 s
5% ΔF/F0
Ca2+ Event Duration (s)
80
60
40
20
0
**
Control
Bf
CCCP
C
90 nM Bf
Thapsigargin (5 μM)
20 s
5% ΔF/F0
Ca2+ Event Duration (s)
80
60
40
20
0
**
**
Control
Bf
Thapsi

592

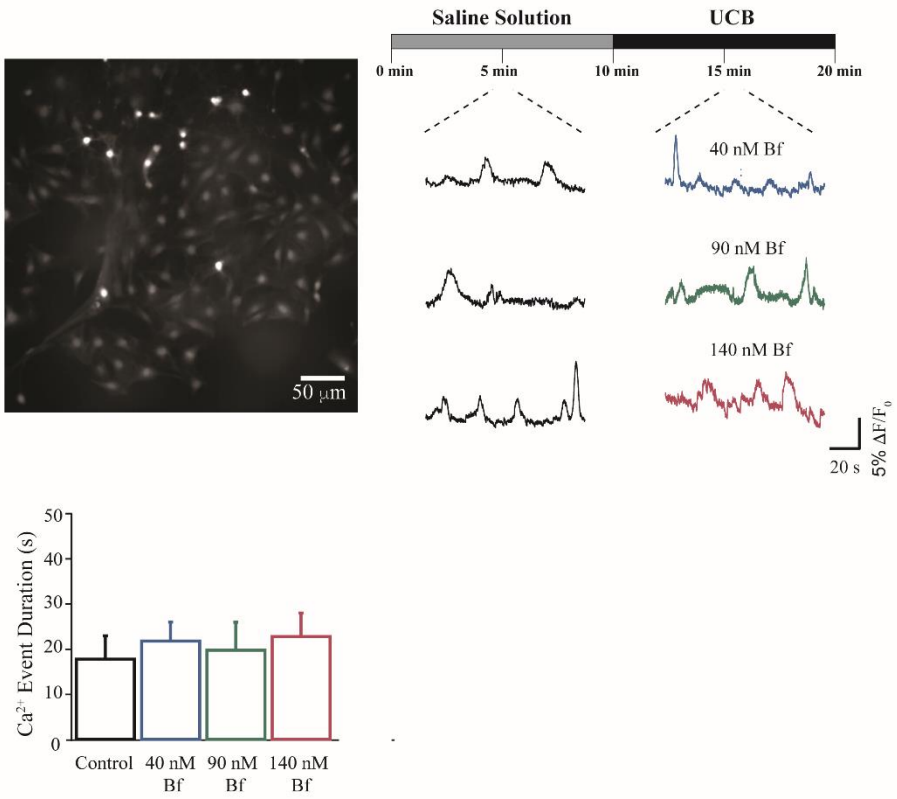
Saline Solution
UCB
0 min
5 min
10 min
15 min
20 min
40 nM Bf
90 nM Bf
140 nM Bf
50 μm
20 s
5% ΔF/F0
Ca2+ Event Duration (s)
0
10
20
30
40
50
Control
40 nM Bf
90 nM Bf
140 nM Bf

593

594

595

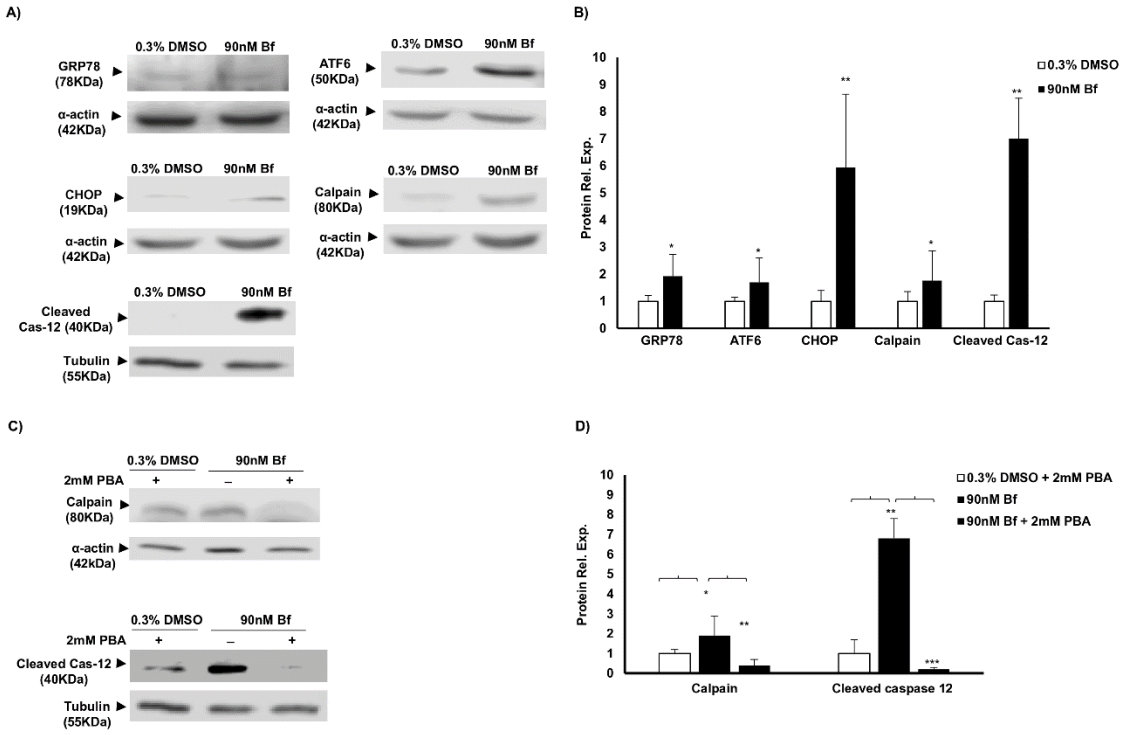
A)
0.3% DMSO
90nM Bf
GRP78 (78KDa)
α-actin (42KDa)
ATF6 (50KDa)
CHOP (19KDa)
Calpain (80KDa)
Cleaved Cas-12 (40KDa)
Tubulin (55KDa)
B)
0.3% DMSO
90nM Bf
Protein Rel. Exp.
GRP78
ATF6
CHOP
Calpain
Cleaved Cas-12
C)
2mM PBA
D)
0.3% DMSO + 2mM PBA
90nM Bf + 2mM PBA
Calpain
Cleaved caspase 12

596

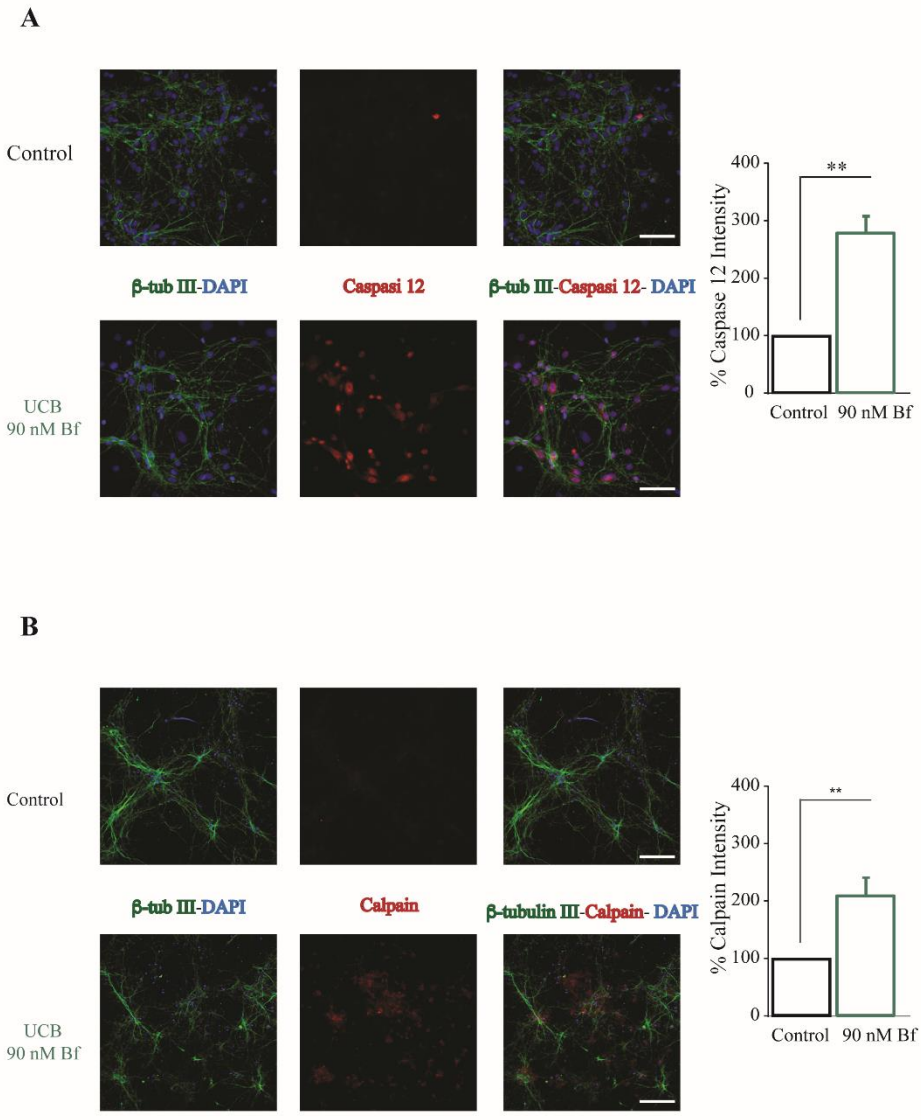
A
Control
β-tub III-DAPI
Caspasi 12
β-tub III-Caspasi 12- DAPI
UCB
90 nM Bf
% Caspase 12 Intensity
400
300
200
100
0
**
Control
90 nM Bf
B
Control
β-tub III-DAPI
Calpain
β-tubulin III-Calpain- DAPI
UCB
90 nM Bf
% Calpain Intensity
400
300
200
100
0
**
Control
90 nM Bf

597

598

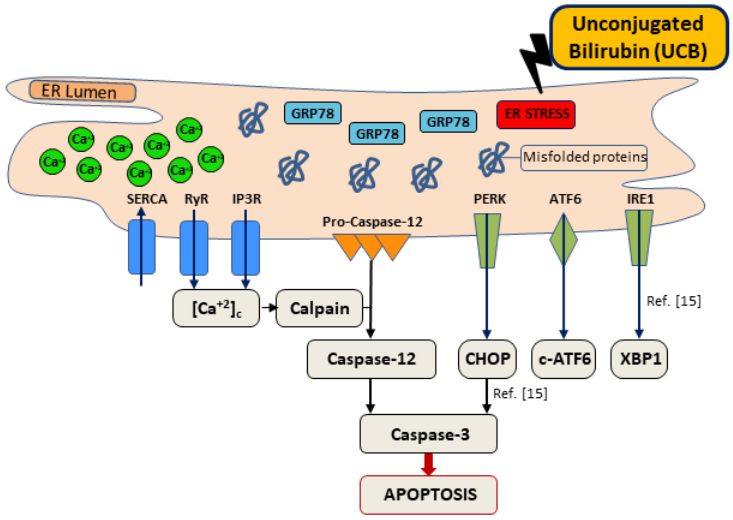
Unconjugated Bilirubin (UCB)
ER Lumen
GRP78
GRP78
GRP78
ER STRESS
Misfolded proteins
SERCA
RyR
IP3R
PERK
ATF6
IRE1
Pro-Caspase-12
[Ca+2]c
Calpain
Ref. [15]
Caspase-12
CHOP
c-ATF6
XBP1
Ref. [15]
Caspase-3
APOPTOSIS

599

Dear Editor,

First, we would like to thank you and the reviewers for the time spent looking over the paper. Based on the evaluation of our manuscript "Bilirubin disrupts calcium homeostasis in neonatal hippocampal neurons: A new pathway of neurotoxicity" (ATOX-D-19-00857), we submit a revised version of the Ms. together with a rebuttal letter dealing with the points raised by the reviewer

Reviewer comments (R) are *in blue italic* while our answers (A) are in black and include the modifications on the revised version of the manuscript. Modifications in the manuscript are highlighted in yellow.

R1. The investigators note that similar effects on calcium dynamics were observed across the original three bilirubin concentrations studied (40 NM, 90 NM, and 140 NM) - whereas the 90 and 140 nM are in the putative toxic range; 40 nM is characterized as "non-toxic" yet had effects similar to those of higher levels -- can the authors please address this observation and how it may impact the assertion that these effect on Ca dynamics are pathologic?

A1: The point raised by the reviewer is well taken. We were also surprised to observe alterations of calcium dynamics at Bf 40 nM, a concentration assumed to be not toxic. The assumption that the threshold of bilirubin toxicity is 70 nM is based on *in vitro* experiments (*Ostrow JD, 2003, Pediatr Res 54:98–104*). The validity of what observed *in vitro* to the *ex vivo* models (in this case) needs to be proven. In addition, Bf determination is influenced by the presence of many factors (FBS, HSA, BSA, chloride, pH) that changes among cell medium used to growth different primary or immortalized cell line. Bf should be measured every time in the same media used experimentally for each different cell type used (*Roca L, 2006, Pediatr Res. Dec;60(6):724-8.*) but this is not common practice. The Bf effect reflects differences in cell type, maturity, function, species of origin. Even if we do not have a clear explanation regarding the Bf 40 nM ability to disrupt calcium homeostasis, we believe that is important to consider that this work was conducted on dissociated primary hippocampal cells from P2-P3 Wistar rats that may be a very sensitive model.

R2. Were these changes in bilirubin-induced Ca dynamics reversible with removal - clearance of bilirubin?

A2: To answer this relevant observation from the reviewer, we have now included in the Supplementary Figure 1S results from a series of experiments where the Ca++ dynamics during bilirubin application and, upon bilirubin removal, washout was monitored for the three different bilirubin concentrations tested. As depicted by the fluorescent traces and summarized in the histograms, 5 min washout did not affected the Ca++ dynamics brought about by 10 min bilirubin application, for all concentrations tested (Bf 40 nM: from 42 ± 6 s to 37 ± 10 s, after 5 min removal, n = 5 cells; Bf 90 nM: from 54 ± 8 s to 51 ± 8 s, after 5 min removal, n= 5 cells; Bf 140 nM: from 50 ± 6 s to 42 ± 8 s, after 5 min removal, n= 4 cells). Conversely, upon 10 min bilirubin washout, a decrease in the Ca++ events' duration was detected (Bf 40 nM: 11 ± 10 s, n = 5 cells; Bf 90 nM: 22 ± 8 s, n = 5 cells; Bf 140 nM: 27 ± 8 s, n= 5 cells), suggestive of a progressive clearance of bilirubin, with the Ca++ event duration resembling that of controls (i.e. prior bilirubin application; see for example Fig 1A or Fig 2A).

R3. Where other concentrations (lower than 40; and higher than 140 nM) studied; how about longer duration of exposures? The in vitro UCB exposures on Ca transients were 40 minutes whereas UCB

effects on Ca dependent apoptotic signaling was 24 hours -- why the different time frames of exposure? How does this impact interpretation of findings?

A3: We did not test concentration lower than 40 or higher that 140 nM. As a pilot study we explored the "canonical Bf concentration" but we agree this will be informative and plan to do it in the future. The reason of the different time frames of exposure deals with the timing of events. Calcium release is a very early and rapid event, while its effect in terms of RNA and protein expression needs a longer time. 24hours is usually considered a good frame time to study RNA and protein expression.

R4. Do the authors have an explanation for the cell specific responses of UCB on Ca transients?

A4: The different impact of UCB on Ca transients between neuronal and glial cells fits with the different toxic effect of UCB in neurons and glial cells. The observation that in astrocytes, the spontaneous glial Ca2+ transients duration was not altered by UCB is in line with our previous demonstration that ER-stress does not occur in U87 astrocytoma cell line despite a intracellular UCB accumulation similar to neuronal cells (15).

R5. Could the authors add a figure detailing the proposed pathophysiology of UCB on neuronal cell Ca dynamics and downstream effects? Would be helpful to the readers

A5: Figure 6 was added to the Ms to explain the proposed mechanism

R6. The authors have previously studied the protective effects of minocycline against UCB neurotoxicity -- minocycline is a known Ca chelator (whereas non Ca chelator minocycline derivatives do not show this neuroprotective property) -- would be of interest in the discussion to visit these effects.

A6) We agree with the comment and we plan to test the direct effect of minocycline on UCB induced calcium oscillations in a near future. A paragraph dealing with the effects of minocycline on UCB neurotoxicity was added to the discussion.

We hope to have comprehensively addressed the critiques raised by the reviewer and we look forward to the acceptance of the revised version.

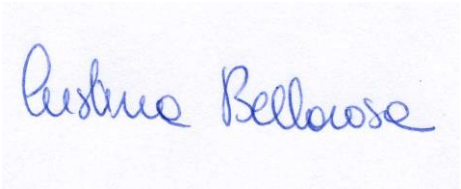

Cristina Bellarosa, PhD
Corresponding author